

UC San Diego

UC San Diego Previously Published Works

Title

Comparison and Design of Servo Controllers for Dual-Stage Actuators in Hard Disk Drives

Permalink

<https://escholarship.org/uc/item/3pk6t9rz>

Journal

IEEE Transactions on Magnetics, 39(5)

ISSN

0018-9464

Author

De Callafon, Raymond

Publication Date

2003-09-01

Peer reviewed

Comparison and Design of Servo Controllers for Dual-Stage Actuators in Hard Disk Drives

Massimiliano Rotunno, Raymond A. De Callafon, and Frank E. Talke, *Senior Member, IEEE*

Abstract—A systematic design procedure is presented that can be used to construct servo controllers for dual-stage actuation in a hard disk drive. The systematic approach is based on optimal control theory using an H_∞ -norm-based control design, where servo design specifications are formulated in terms of relatively simple weighting functions. Different possible servo control strategies are designed and compared on performance and energy consumption. Results based on a piezoelectric milli-actuator from Hutchinson Technology Inc. illustrate the design of a dual-stage servo controller that is able to perform high-density track recording, with a significant reduction in power consumption.

Index Terms—Digital control, hard disks, optimal control, servosystems.

I. INTRODUCTION

HIGH track densities in hard disk drives (HDDs) with perpendicular media can be obtained by using dual-stage actuation, where the coarse actuation of the voice coil motor (VCM) is accompanied with an additional micro- or milli-actuator. The dual-stage actuator is positioned in close proximity of the read/write head and exhibits favorable properties associated with collocated control.

The design of servo controllers for track following with dual-stage actuators in an HDD has been an active area of research. Intuitive approaches based on loop shaping of the VCM and dual-stage control loops [1]–[3] have provided satisfactory results. However, most of these approaches require many design iterations to include necessary control objectives. These objectives may include pole and zero locations of servo controller and shape of the resulting closed-loop transfer functions. An alternative is to use an optimal control design method [4]–[7] that uses optimization techniques to tune the servo controller. As the computation of the controller is done via an optimization, the design process can be automated. Finally, the use of an H_∞ -norm based optimal control design allows robustness issues to be incorporated into the dual-stage servo control design relatively easily.

This paper builds on the techniques used in optimal control design to come up with a systematic approach to design

a dual-stage servo controller. The systematic design approach presented in this paper only requires the specification of the shape of well-defined weighting functions, that are directly related to the shape of closed-loop transfer functions of interest. Compared to the approaches mentioned in [4]–[7], this paper lists a systematic way of choosing weighting functions to set up the dual-stage control problem. With the use of this systematic approach, different dual-stage control configurations are compared and the advantages of a dual-stage actuator are illustrated for a Magnum 5e piezoelectric milli-actuator provided in 2000 by Hutchinson Technology Inc. (HTI), Hutchinson, MN.

II. SERVO CONTROLLER CONFIGURATIONS

In order to study the benefits of a dual-stage actuator, both the control of the single VCM and the dual-stage control are presented in this paper. Using the notation P_{vcm} to indicate a dynamical model of the VCM with the flexibilities of the E-block and suspension, the reduction of track misregistration in a single stage VCM control is characterized by the sensitivity function

$$S_{\text{vcm}} = \frac{1}{1 + P_{\text{vcm}}C_{\text{vcm}}} \quad (1)$$

where C_{vcm} is used to denote the single-stage VCM servo controller.

When an additional milli-actuator P_{ma} is added to the control loop, the rejection of track misregistration can be characterized by

$$S_{\text{dual}} = \frac{1}{1 + PC} = \frac{1}{1 + P_{\text{ma}}C_{\text{ma}} + P_{\text{vcm}}C_{\text{vcm}}} \quad (2)$$

where the notation $P = [P_{\text{ma}} \ P_{\text{vcm}}]$ and $C = [C_{\text{ma}} \ C_{\text{vcm}}]^T$ are used to denote the dynamical models of the dual-stage actuator P and dual-stage controller C . High servo bandwidth control using the dual-stage actuator can provide better disturbance rejection than with the single-stage VCM servo configuration. Intuitively, this can be seen by rewriting (2) into

$$S_{\text{dual}} = S_{\text{vcm}} \left(1 - \frac{P_{\text{ma}}C_{\text{ma}}}{1 + P_{\text{ma}}C_{\text{ma}} + P_{\text{vcm}}C_{\text{vcm}}} \right)$$

where S_{vcm} is given in (1). Hence, the additional design freedom of the product $P_{\text{ma}}C_{\text{ma}}$ (milli-actuator loop gain) can be used to make $S_{\text{dual}} \leq S_{\text{vcm}}$. Moreover, the small inertia of the milli-actuator P_{ma} will translate to a much smaller power consumption in the case where high bandwidth servo control is desired.

The dual-stage controller C produces two control outputs from a single position error signal (PES) measurement. No independent measurements of the output of the actuators P_{vcm} and

Manuscript received January 22, 2003.

M. Rotunno was with the Mechanical and Aerospace Engineering Department, University of California at San Diego, La Jolla, CA 92093-0411 USA. He is now with Aerostudi SpA, 00122 Rome, Italy (e-mail: rd.rm@aerostudi.com).

R. A. De Callafon is with the Mechanical and Aerospace Engineering Department, University of California at San Diego, La Jolla, CA 92093-0411 USA (e-mail: callafon@ucsd.edu).

F. E. Talke is with the Center for Magnetic Recording Research, University of California at San Diego, La Jolla, CA 92093-0401 USA (e-mail: ftalke@ucsd.edu).

Digital Object Identifier 10.1109/TMAG.2003.816491

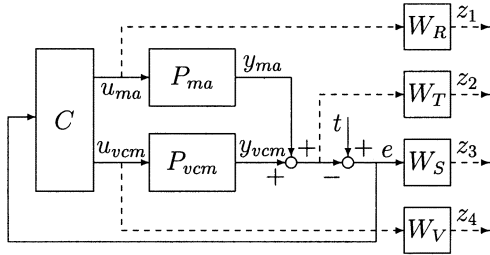


Fig. 1. Feedback connection of milli-actuator P_{ma} and VCM P_{vcm} with closed-loop weighting functions W_R , W_T , W_S , and W_V .

P_{ma} are available, and destructive interference can occur. With (2), it can be seen that the interference occurs at those points $s \in \mathcal{C}$ where $P_{ma}(s)C_{ma}(s) + P_{vcm}(s)C_{vcm}(s) = 0$. These points constitutes zeros of the closed-loop system that are being introduced in the dual-stage servo controller configuration. To avoid the introduction of (low frequent) lightly damped zeros in the closed-loop system, frequency separation can be used.

III. SYSTEMATIC CONTROLLER DESIGN

A. Definition of Weighting Functions

The control design approach is based on standard H_∞ optimization and only the specification of well-defined closed-loop weighting functions depicted in Fig. 1. The desired shape of the sensitivity function $S := S_{dual}$ in (2) is captured by the weighting function W_S . The design of the controller C should be done such that $\|W_S S\|_\infty < 1$ to guarantee that the sensitivity function S is bounded from above by the desired shape W_S^{-1} . The transfer function from track t to output $y_{ma} + y_{vcm}$ is given by the complimentary sensitivity $T = P(1 + CP)^{-1}C$ and in order to restrict the overall control energy, the shape of T will be bounded by $\|W_T T\|_\infty < 1$.

Frequency separation is enabled by the weighting functions W_R and W_V . The weighting function W_V is used to bound the (high frequency) control signal of the VCM via $\|W_V C_{vcm} S\|_\infty < 1$. For the VCM controller configuration, W_R is set to be $W_R = 0$ and for the dual-stage configuration depicted in Fig. 1, W_R is used to weigh the input u_{ma} of the milli-actuator by requiring $\|W_R C_{ma} S\|_\infty < 1$.

B. Shape of Weighting Functions

In order to achieve disturbance rejection of the nonrepeatable runout errors and a sufficient bandwidth for track following, the weighting function W_S^{-1} is chosen as a high-pass filter

$$W_S^{-1}(s) := \frac{\left(\frac{s}{\sqrt{M_S}} + \omega_S\right)^2}{(s + \omega_S \sqrt{A_S})^2}. \quad (3)$$

The filter W_S in (3) is parametrized by: A_S for the desired low frequency attenuation and steady-state error, M_S to bound the maximum peak of S , and ω_S that specifies the cutoff frequency of the high-pass filter. Setting $A_S = 0$ yields a double integrator in W_S and provides integral action in the servo controller C . Selection of $M_S < 2$ guarantees a gain margin > 6 dB and a phase margin $> 30^\circ$, whereas ω_S is related to the closed-loop bandwidth.

To restrict the overall control energy by having sufficient roll off at high frequencies, W_T^{-1} is a second-order low-pass

$$W_T^{-1}(s) := \frac{\left(\frac{s}{\sqrt{A_T}} + \omega_T\right)^2}{(s + \omega_T \sqrt{M_T})^2} \quad (4)$$

parameterized via the parameters A_T to specify the high frequency attenuation, M_T to bound the maximum peak of T and ω_T to determine the cutoff frequency.

The weighting functions W_R and W_V are used to achieve frequency separation by distributing the control energy. Due to the small inertia and high resonance modes of the milli-actuator, the milli-actuator can operate at high frequencies, whereas the VCM should be configured to track relatively low-frequency signals. This can be achieved by choosing W_R^{-1} as a first-order high-pass filter

$$W_R^{-1}(s) := \frac{\frac{s}{M_R} + \omega_R}{s + \omega_R A_R} \quad (5)$$

where the parameters M_R , A_R , and ω_R are similar to the design parameters used in W_S . With W_R specified as a high-pass filter, it suffices to choose W_V as a constant weighting filter to limit the maximum peak of the transfer function from track input t to VCM control input u_{vcm} . It should be noted that the parameterizations above are given in terms of continuous time transfer functions and can be converted to discrete-time filters via a bilinear transformation.

C. H_∞ Synthesis

The combination of weighting functions and design specifications requires the design of a controller C such that $\|W_S S\|_\infty < 1$, $\|W_T T\|_\infty < 1$, $\|W_V C_{vcm} S\|_\infty < 1$, and $\|W_R C_{ma} S\|_\infty < 1$. Such a design can be performed via a standard H_∞ synthesis [8], [9] for which the model and weighting functions are combined in a generalized plant

$$\begin{bmatrix} z_1 \\ z_2 \\ z_3 \\ z_4 \\ e \end{bmatrix} = \begin{bmatrix} 0 & W_R & 0 \\ 0 & W_T P_{ma} & W_T P_{vcm} \\ W_S & -W_S P_{ma} & -W_S P_{vcm} \\ 0 & 0 & W_V \\ 1 & -P_{ma} & -P_{vcm} \end{bmatrix} \begin{bmatrix} t \\ u_{ma} \\ u_{vcm} \end{bmatrix}. \quad (6)$$

With the generalized plant in (6), standard H_∞ optimization techniques can be used to synthesize a controller C that minimizes γ in $\|T_{zw}\|_\infty < \gamma$ where T_{zw} is the transfer function from $w = t$ to $z = [z_1 \ z_2 \ z_3 \ z_4]^T$. From (6), it can be observed that

$$T_{zw} = [W_S S \quad W_T T \quad W_V C_{vcm} S \quad W_R C_{ma} S]^T \quad (7)$$

and includes all the design transfer functions. Finding a controller C that yields $\gamma \leq 1$ indicates that nominal performance is satisfied and the design specifications $\|W_S S\|_\infty < 1$, $\|W_T T\|_\infty < 1$, $\|W_V C_{vcm} S\|_\infty < 1$, and $\|W_R C_{ma} S\|_\infty < 1$ have been met.

IV. APPLICATION TO DUAL-STAGE ACTUATOR

A. Model and Weighting Function Selection

To illustrate the design procedure and show the favorable properties of a dual-stage actuator, a model of the Magnum 5e suspension, manufactured by HTI is used. The model of the

TABLE I
 CLOSED-LOOP WEIGHTING FUNCTION PARAMETERS

| Weight | ω [rad/s] | M [-] | A [-] |
|--------|-------------------|---------|---------|
| W_S | $1000 \cdot 2\pi$ | 2 | $1e-6$ |
| W_R | $100 \cdot 2\pi$ | 10 | $1e-3$ |
| W_T | $7000 \cdot 2\pi$ | 1.7 | $1e-3$ |

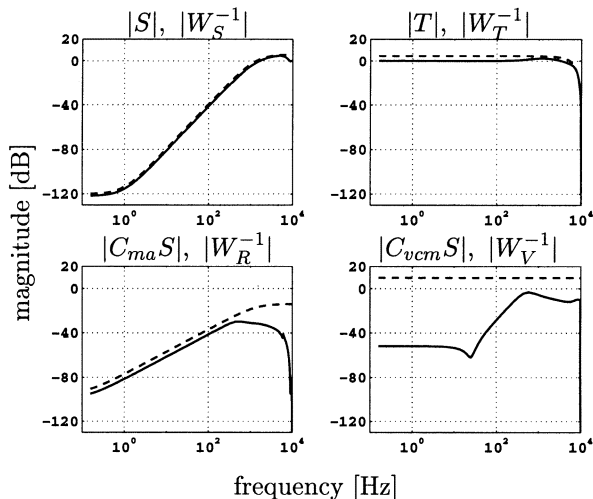


Fig. 2. Closed-loop transfer functions (solid) and (inverse of) corresponding weighting functions (dashed) used in the dual-stage design.

VCM actuator P_{vcm} is an eighth-order model, composed of a VCM mode (lightly damped free body mode) at 25 Hz, an E-block mode at 5 kHz, a suspension torsion mode at 5.9 kHz, and a suspension sway mode at 9 kHz. The milli-actuator model P_{ma} is a fourth-order model which includes the dominant suspension torsion and sway modes.

The choice for the parameters of the weighting functions W_S , W_T , and W_R are given in Table I, whereas W_V is chosen to be $W_V = 0.33$. It can be observed from Table I that the parameters are chosen such that the lower bound on the bandwidth is specified as 1 kHz, whereas the high-frequency rolloff is specified to start at 7 kHz.

B. Control Design Results

The H_∞ synthesis of [9] yields a stable eighth-order controller C with $\|T_{wz}\|_\infty < 1$ and, thus, the nominal performance condition has been met. This has been illustrated in Fig. 2 where amplitude Bode plots of the various closed-loop transfer functions and the corresponding weighting functions are given.

To illustrate the frequency separation obtained by the designed dual-stage controller, in Fig. 3 a simulated 1- μm step response of the dual-stage closed-loop system has been depicted. The first part of the step response y is dominated by the fast response of the milli-actuator and the slower response of the VCM brings the relative displacement between the two actuators back to zero.

C. Implementation and Comparison of Controllers

A single-stage VCM controller was designed to obtain a maximum bandwidth, given the limitations on the control signal

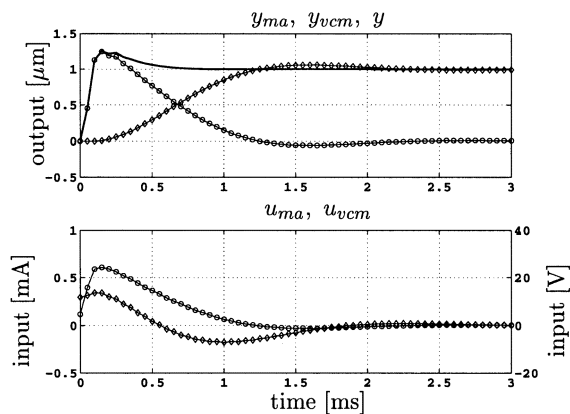

 Fig. 3. Simulated step response data with dual-stage controller: top figure shows actuator output signals $y = y_{ma} + y_{vcm}$ (solid), y_{ma} (\circ), y_{vcm} (\diamond); bottom figure shows actuator control signals u_{ma} (\circ), u_{vcm} (\diamond).

 TABLE II
 COMPARISON OF CONTROLLER CONFIGURATIONS

| TYPE | BW (kHz) | GM (dB) | PM (deg) | $\ u_{vcm}\ _2$ | $\ u_{ma}\ _2$ |
|--------|----------|---------|----------|-----------------|----------------|
| single | 0.45 | 8.8 | 39 | 9.5 | — |
| dual | 1.1 | 8.1 | 38 | 0.3 | 0.015 |

u_{vcm} of the VCM. With an LDV measurement of the PES sampled at 20 kHz, both a single-stage and a dual-stage servo controller were implemented on a spinstand with a VCM and a Magnum 5e dual-stage suspension. The bandwidth (BW), gain margin (GM), phase margin (PM), and the variance of the control signals were estimated using time- and frequency-domain analysis and are displayed in Table II. A larger bandwidth and smaller control signals are obtained with the dual-stage controller using the frequency separation design.

REFERENCES

- [1] S. Schroeck and W. Messner, "On controller design for linear time-invariant dual-input single-output systems," in *Proc. American Control Conf.*, San Diego, CA, June 1999, pp. 4122–4126.
- [2] L. Guo, D. Martin, and D. Brunnet, "Dual-stage actuator servo control for high density disk drives," in *Proc. IEEE/ASME Int. Conf. Advanced Intelligent Mechatronics*, Atlanta, GA, Sept. 1999, pp. 132–137.
- [3] T. Semba, T. Hirano, J. Hong, and L. Fan, "Dual-stage servo controller for HDD using MEMS microactuator," *IEEE Trans. Magn.*, vol. 35, pp. 2271–2273, Sept. 1999.
- [4] D. Hernandez, S. Park, R. Horowitz, and A. Packard, "Dual-stage track-following servo design for hard disk drives," in *Proc. American Control Conf.*, San Diego, CA, June 1999, pp. 4116–4121.
- [5] D. Horsley, D. Hernandez, R. Horowitz, A. Packard, and A. Pisano, "Closed-loop control of a microfabricated actuator for dual-stage hard disk drive servo systems," in *Proc. American Control Conf.*, Philadelphia, PA, June 1998, pp. 3028–3032.
- [6] R. de Callafon, D. Harper, R. Skelton, and F. Talke, "Experimental modeling and feedback control of a piezo-based milliactuator," *J. Inform. Storage Process. Syst.*, vol. 1, pp. 1–8, 1999.
- [7] W. Guo and J. Bozorgi, "Dual-stage servo systems with microactuated head gimbal assemblies," *J. Inform. Storage Process. Syst.*, vol. 2, no. 1/2, pp. 101–108, 2000.
- [8] K. Zhou and J. Doyle, *Essentials of Robust Control*. Upper Saddle River, NJ: Prentice-Hall, 1998.
- [9] M. Rotunno and R. de Callafon, "A bundle method for solving the fixed order control problem," in *Proc. 41st IEEE Conf. Decision and Control*, Las Vegas, NV, 2002, pp. 3156–3161.